Self-assembly of a novel mixed-valence tetranuclear molecular square $[Fe^{II}_3Fe^{III}L_2(HL)_2]^{3+}$ and $[M(HL)]_4^{4+}$ squares (M = Ni, Zn and Cd) {H_2L = bis(2-acetylpyridine) thiocarbazone}

Han Gang, Guo Dong, Duan Chun-Ying,* Mo Hong and Meng Qing-jin

Coordination Chemistry Institute, The State Key Laboratory of Coordination Chemistry, Nanjing University, Nanjing 210093, P.R.China. E-mail: duancy@nju.edu.cn

Received (in Montpellier, France) 18th April 2002, Accepted 14th June 2002
First published as an Advance Article on the web 22nd August 2002

A novel mixed-valence rigid molecular square $[Fe^{II}_3Fe^{III}L_2(HL)_2]^{3+}$ was constructed *via* self-assembly using bis(2-acetylpyridine) thiocarbazone (H_2L) as both linker and reducing agent. Single crystal structure analysis shows that each cation is located at an inversion center with four iron atoms at the corners of a square with edge length Fe···Fe *ca.* 4.2 Å. Magnetic measurement exhibits that there is only one Fe^{III} center in each of the tetranuclear squares. There is no significant difference of the coordinated bonds among the four iron centers, indicating that it is impossible to recognize the Fe^{III} in the four iron centers of a square. Electrochemical measurement and UV–VIS–NIR spectral studies demonstrate the Robin–Day class II behavior of the mixed-valence compound with appreciable iron–iron interaction. New rigid metallocyclic squares $[Ni(HL)]_4^{4+}$, $[Zn(HL)]_4^{4+}$ and $[Cd(HL)]_4^{4+}$ were also assembled and structurally characterized for comparison. ESI-MS spectra reveal that the fragments of tetranuclear molecular squares are stable even in solution.

Introduction

Due to a variety of special functional properties such as luminescence,[1] redox activity[2] and magnetism,[3] the latest decade has witnessed the rapid burgeoning field of conformational rigid, novel, tetranuclear geometric metallocyclic squares, characterized by *ca.* 90° bond angles around each corner atom, by self-assembly of the component metal complexes.[4–6] Recently, we have been interested in designing new metallocyclic squares using the cheap, easy-to-prepare thiocarbazone derivatives containing pyridine motif as linkers.[7] Such systems have potential applications in biological and material science, since thiosemicarbazone and thiocarbazone belong to a large group of thiourea derivatives whose biological activities are a function of the parent aldehyde or ketone.[8–10] Studies also show that thiosemicarbazones and their metal complexes have potential applications in non-linear optical materials.[11] To obtain squares that are robust enough to survive both in the solid and solution, and to study the potential biological properties of such squares, here we use bis(2-acetylpyridine) thiocarbazone[12] (H_2L) to construct rigid metal based cationic molecular squares.

On the other hand, the properties of inorganic mixed-valence (MV) compounds have been extensively investigated,[13–15] because of their potential application to energy conversion, information storage and photocatalysis. Here, Fe^{III} is used to create a mixed-valence $Fe^{II}_3Fe^{III}$ square. Such a study on a mixed-valence complex based molecular square has not been reported to the best of our knowledge.

Experimental

General

Bis(2-acetylpyridine) thiocarbazone (H_2L) was prepared according to the published method.[12] IR spectra were recorded on a Nicolet 170SX FT-IR spectrophotometer with KBr discs in the range 4000–400 cm^{-1}, UV–VIS–NIR spectra were recorded on a Shimadzu UV-3100 spectrometer. ^1H NMR spectra were recorded on Am500 Bruker spectrometers at 298 K using TMS as the internal standard. Magnetic measurements were carried out on powder samples with a CHAN 2000 Faraday-type magnetometer in the temperature range 75–300 K. Electrospray mass spectra were recorded on a LCQ system (Finnigan MAT, USA) using methanol as the mobile phase. Elemental analyses of carbon, nitrogen and hydrogen were performed on a Perkin-Elmer 240 analytical instrument. Pulse voltammograms were recorded on an EG&G M273 potentiostat/galvanostat system using a glass-carbon working electrode, a platinum wire counter electrode and an Ag/AgCl reference electrode. Measurements were carried out in acetonitrile solution containing 0.1 M tetrabutylammonium perchlorate as supporting electrolyte at a scan rate of 30 mV s^{-1}. Ferrocene (1.0×10^{-3} mol dm^{-3}) was used as an external standard with $E_{1/2} = 0.46$ V *vs.* Ag/AgCl electrode.

Syntheses

$[Ni(HL)]_4[PF_6]_4$ 1. Bis(2-acetylpyridine)thiocarbazone H_2L (0.16 g, 0.5 mmol) and $NiCl_2\cdot6H_2O$ (0.12 g, 0.5 mmol) were mixed in 15 ml methanol. After refluxing for 1 h and cooling to room temperature, KPF_6 (0.18 g, 1.0 mmol) was added and refluxing was resumed for 3 h. The brown precipitate formed was isolated and recrystallized from acetonitrile–ethanol (1:1). Yield 80% (Found: C, 35.5; H, 3.7; N, 15.9; Calc. for $C_{60}N_{24}H_{60}S_4Ni_4P_4F_{24}\cdot CH_3CH_2OH$: C, 35.4; H, 3.2; N, 16.0%). IR (cm^{-1}): 3423, 3344 (ν_{C-H}); 2964, 2924 (ν_{N-H}); 1603, 1563, 1518, 1468, 1443 ($\nu_{C=C}$, ν_{C-N}); 1260 (ν_{N-N}); 1153 (ν_{C-S}); 843(s) (ν_{P-F}); 776, 744 (δ_{C-H}). Crystals suitable for crystal determination were obtained by slowly evaporating an acetonitrile–ethanol (1:1) solution in air.

$[Zn(HL)]_4[BF_4]_4$ 2 and $[Cd(HL)]_4[BF_4]_4$ 3. Bis(2-acetylpyridine) thiocarbazone H_2L (0.16 g, 0.5 mmol) and $M(BF_4)_2$

DOI: 10.1039/b203819f

(0.5 mmol) (M = Zn or Cd) were mixed in 15 ml methanol. After stirring for 3 h, the yellow precipitate formed was isolated. For complex **2**: yield 90% (Found: C, 37.7; H, 4.2; N, 15.9; Calc. for $C_{60}N_{24}H_{60}S_4Zn_4B_4F_{16}\cdot6CH_3OH\cdot4H_2O$: C, 37.4; H, 4.4; N, 15.9%). IR (cm^{-1}): 3424, 3269 ($\nu_{C\text{–}H}$); 3066, 2920 ($\nu_{N\text{–}H}$); 2920, 1594, 1563, 1521, 1471, 1441 ($\nu_{C=C}$, $\nu_{C\text{–}N}$); 1257 ($\nu_{N\text{–}N}$); 1153 ($\nu_{C\text{–}S}$); 1074 ($\nu_{B\text{–}F}$); 779 (m), 744 (m) ($\delta_{C\text{–}H}$). ^{1}H NMR: $\delta_H[(CD_3)_2SO]$: 2.51 (24H, s, CH_3), 6.01 (4H, br, NH); 7.51 (8H, t, py); 7.68 (8H, d, py); 8.01 (8H, t, py); 8.74 (8H, d, py). For complex **3**: yield 88% (Found: C, 32.7; H, 3.8; N, 13.6; Calc. for $C_{60}N_{24}H_{60}S_4Cd_4B_4F_{16}\cdot CH_3OH_6\cdot6H_2O$: C, 33.1; H, 4.3; N, 14.0%). IR (cm^{-1}): 3484, 3268 ($\nu_{C\text{–}H}$), 3018, 2924 ($\nu_{N\text{–}H}$); 1593, 1563, 1520, 1471, 1439 ($\nu_{C=C}$, $\nu_{C\text{–}N}$); 1251 ($\nu_{N\text{–}N}$); 1147 ($\nu_{C\text{–}S}$); 1072 ($\nu_{B\text{–}F}$); 785, 734 ($\delta_{C\text{–}H}$). ^{1}H NMR: $\delta_H[(CD_3)_2SO]$: 2.51 (24H, s, CH_3); 6.00 (4H, br, NH); 7.39 (8H, t, py), 7.86 (8H, d, py); 8.15 (8H, t, py) and 8.58 (8H, d, py). Crystals suitable for crystal determination were obtained by slowly evaporating acetonitrile–ethanol (1:1) solutions in air.

$[Fe_4(HL)_2L_2][FeCl_4]_3$ 4. Bis(2-acetylpyridine)thiocarbazone H_2L (0.16 g, 0.5 mmol) and $FeCl_3\cdot6H_2O$(0.13 g, 0.5 mmol) were mixed in 15 ml methanol. After refluxing for three hours, dark precipitate formed was isolated. Yield 80%. Found: C, 33.8; H, 3.6; N, 13.4; Calc. for $C_{60}N_{24}H_{58}S_4Fe_4Fe_3Cl_{12}\cdot((CH_3OH)_8\cdot(H_2O)_4$: C, 34.2; H , 4.1; N, 14.1 %.IR (cm^{-1}): 3422 ($\nu_{C\text{–}H}$), 3075 ($\nu_{N\text{–}H}$), 1595, 1565, 1541, 1466, 1417($\nu_{C=C}$, $\nu_{C\text{–}N}$); 1146 ($\nu_{C\text{–}S}$); 1262 ($\nu_{N\text{–}N}$); 771, 743 ($\delta_{C\text{–}H}$).Crystals suitable for crystal determination were obtained by slowly evaporating benzene solution in air.

Crystallography

Parameters for data collection and refinement of the complexes are summarized in Table 1. Intensities of complex **1, 2** and **4** were collected on a Siemens SMART–CCD diffractometer with graphite-monochromated Mo-Kα radiation (λ = 0.71073 Å) using SMART and SAINT programs.[16] The structures were solved by direct methods and refined on F^2 using full-matrix least-squares methods using SHELXTL version 5.1.[17] Anisotropic thermal parameters were refined for non-hydrogen atoms for complexes **1, 2** and **4**. The PF_6^- anions in the crystal structure of **1**, the BF_4^- anions in the crystal structure of **2**, and the $FeCl_4^-$ anions in complex **4** as well as one of the ligands in the crystal structure of **2** and solvent molecules in all of the three crystal structures were refined disordered. The site occupancy factors about the two disordered parts were determined using free variables. Distance restrains and thermal parameter restrains were used to make the refinement of part of the disordered atoms stable. Hydrogen atoms were located geometrically and refined using a riding model. Owing to the presence of widespread disorder in the structures, the consequence of the treatments and refinements may well propagate to some extent to the values of all structural parameters beyond those pertaining to the disordered parts, so limiting the validity of detailed comparisons. However, such treatments of the structure refinements are helpful in understanding the chemistry of those systems.

CCDC reference numbers 190867–190869. See http://www.rsc.org/suppdata/nj/b2/b203819f/for crystalliographic data in CIF or other electronic format.

Results and discussion

ESI-MS for complexes 1, 2 and 3

Copper(II) and zinc(II) complexes of bis(2-acetylpyridine) thiocarbazone H_2L have been synthesized by simply mixing the ligand and metal salt in ethanol solution, respectively, however, no molecular boxes have been reported based on the ligand.[12] Reaction of bis(2-acetylpyridine) thiocarbazone H_2L with Ni^{II} salt yields a metal-assisted molecular cation $[Ni(HL)]_4^{4+}$. ESI-MS spectrum of complex **1** (Fig. 1) in methanol reveals the presence of four main peaks: the base peak at m/z 369.3 in which the isotopic distribution patterns separated by 0.25 ± 0.1 dalton, assigned to the most abundant ion $[Ni_4(HL)_4]^{4+}$, peaks at 493.1 and 738.1 resulting from the $[Ni_4L(HL)_3]^{3+}$ and $[Ni_4L_2(HL)_2]^{2+}$, respectively, and a peak at m/z 1477.1 assigned to the species $[Ni_4L_3(HL)]^+$. The presence of the $[Ni(HL)_n(L)_{4-n}]^{n+}$ (n = 1, 2, 3 and 4) species indicates that $[Ni_4(HL)_4]^{4+}$ can lose one, two or three hydrogen atoms from the ligands under the electrospraying condition, and no species corresponding to the fragments result from loss of metal ions and ligands. It can be seen from the ESI-MS spectrum that the tetranuclear complex is the only species in solution, and the square structure of tetranuclear molecular fragment is very stable in solution.

The ESI-MS of tetranuclear square **2** shows five main peaks at m/z 377.1 564.1, 751.1, 1126.8 and 1498.9, assigned to $[Zn_4(HL)_4]^{4+}$, $[Zn_3(L)(HL)_2]^{2+}$, $[Zn_4(L)_2(HL)_2]^{2+}$, $[Zn_3(L)_2(HL)]^+$ and $[Zn_4(L)_3(HL)]^+$, respectively. ESI-MS of complex **3** displays six main peaks, four peaks with m/z of 423.7, 564.8, 844.6 and 1691.7 assigned to $[Cd_4(HL)_4]^{4+}$,

Table 1 Crystallographic data for compounds **1**, **2** and **4**

Compound	**1**·H_2O	**2**·0.5H_2O	**4**·H_2O·1.5C_6H_6
Molecular formula	$C_{60}H_{62}N_{24}P_4F_{24}S_4Ni_4O$	$C_{60}H_{61}N_{24}B_4F_{16}O_{0.5}S_4Zn_4$	$C_{69}H_{69}N_{24}Cl_{12}S_4Fe_7O$
M	2078.30	1918.28	2195.09
Crystal system	Monoclinic	Triclinic	Monoclinic
Space group	$P2_1/n$	$P\bar{1}$	$C2/c$
a/Å	14.563(6)	13.448(5)	31.619(2)
b/Å	40.993(16)	14.955(5)	20.491(1)
c/Å	15.378(6)	21.554(7)	29.755(2)
α/°		87.124(6)	
β/°	100.376(8)	80.677(6)	102.64(1)
γ/°		71.389(6)	
V/Å^3	9030(6)	4054(2)	18 810(2)
Z	4	2	8
T/K	293	293	293
μ/mm^{-1}	1.086	1.363	1.532
Unique reflections	11 779 (R_{int} = 0.131)	10 518 (R_{int} = 0.076)	12 282 (R_{int} = 0.068)
R_1	0.078	0.079	0.068
wR_2 (all data)	0.130	0.140	0.177
Goodness of fit	1.012	0.998	0.918

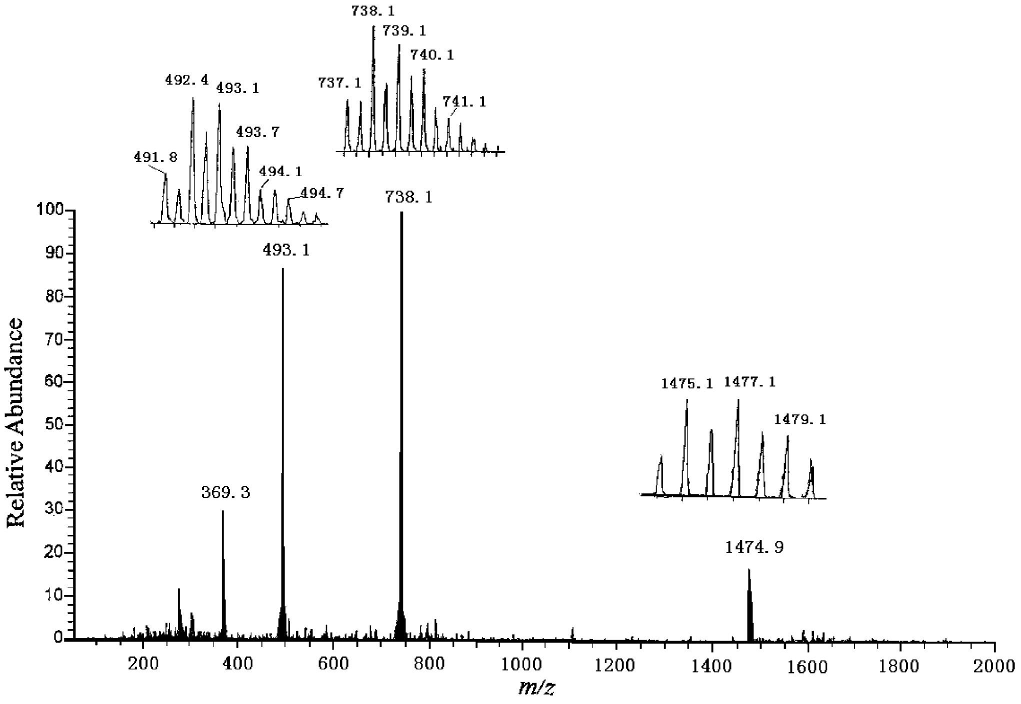

Fig. 1 Electrospray mass spectrum of complex **1** in methanol; the inserts show the isotopic distributions for the main peaks.

$[Cd_4L(HL)_3]^{3+}$, $[Cd_4L_2(HL)_2]^{2+}$ and $[Cd_4L_3(HL)]^{+}$, respectively, like those of nickel complex **1**. The other peaks with m/z 635.5, 1270.7, correspond to the species $[Cd_3L(HL)_2]^{2+}$ and $[Cd_3L_2(HL)]^{+}$, respectively. The presence of the $[M_3L(HL)_2]^{2+}$ and $[M_3L_2(HL)]^{+}$ species indicates that the $[M(HL)_n(L)_{4-n}]^{n+}$ cations may lose one metal ion under electrospraying condition.

Crystal structures of complexes 1 and 2

X-Ray crystallographic studies have unequivocally confirmed the existence of tetranuclear cationic molecular squares of **1** and **2** (Fig. 2). The cation is formed by four metal ions and four deprotonated ligands HL^- with the metal atoms at the corners of a square with edge length M···M separation ranges from 4.64 to 4.71 Å. The sulfur atoms, the thiocarbazone nitrogen atoms and the pyridine nitrogen atoms from the two different ligands octahedrally coordinate to each metal center. These two ligands bond to one metal center in the *mer* configuration (with pairs of sulfur atoms and pyridine nitrogen atoms each bearing a *cis*-relationship, whereas the thiocarbazone nitrogen atoms are *trans* to each other), as found in related octahedrally coordinated metal thiocarbazone and thiosemicarbazone.[7] The sulfur atoms lie at the mid-points of the edges of square, each being connected to two metal atoms with average M–S–M and S–M–S bond angles of about 155 and 93°, respectively. While the free ligand H_2L is in the *E*–*Z* form for the thiocarbazone moiety,[12] on complexation it rearranges to the *Z*–*Z* conformation to make the Schiff-base nitrogen atoms, pyridinyl nitrogen atoms and the sulfur atoms all placed on the same side. This enables the ligand to function as a planar N_5S anionic ligand. For complex **1** (Table 2), the C–S bond lengths of about 1.71–1.73 Å for S(1)–C(8), S(3)–C(38) and S(4)–C(53), are within the normal range of a C–S bond, indicating that the moiety HL^- adopts the thiol tautomeric form acting as a mono-negative ligand. The C–N and N–N bond distances in HL^- are intermediate between formal single and double bonds, pointing to extensive delocalization over the entire molecular skeleton and to effects of disordered distribution of the protonated nitrogen sites in the ligand. The thiocarbazone hydrogen atoms of the mono-anions HL^- could not be located from the difference Fourier map, and are most likely disordered over the imino-nitrogen atoms. Bond distances about 1.40, 1.39 and 1.36 Å for C(8)–N(14), C(38)–N(33) and C(53)–N(44), indicating predominant single bond character for such C–N bonds, and bond distances about 1.30 Å for C(8)–N(13), C(38)–N(34) and C(53)–N(43), indicating prevalent double bond character for those C=N bonds. It seems that the nitrogen atoms N(14), N(33) and N(44) are preferentially protonated. The C–S bond length of about 1.67 Å for S(2)–C(23) suggest that the moiety HL^- adopts the thione tautomeric form acting as a mono-negative ligand, and the thiocarbazone hydrogen atom is most likely disordered over

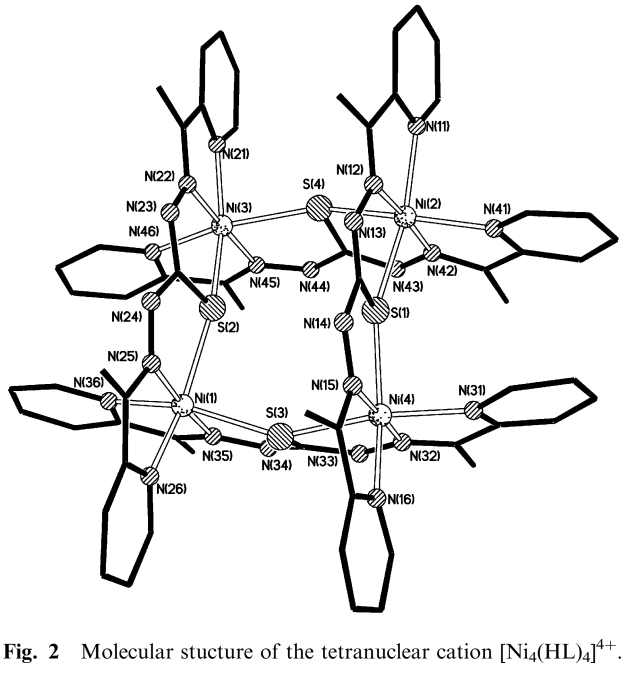

Fig. 2 Molecular stucture of the tetranuclear cation $[Ni_4(HL)_4]^{4+}$.

Table 2 Selected bond lengths (Å) and angles (°) for complex $\mathbf{1}\cdot H_2O$

Ni(1)–S(2)	2.388(2)	Ni(2)–S(1)	2.398(2)	Ni(3)–S(2)	2.379(2)
Ni(1)–S(3)	2.394(2)	Ni(2)–S(4)	2.409(2)	Ni(3)–S(4)	2.379(2)
Ni(1)–N(25)	2.009(5)	Ni(2)–N(11)	2.094(5)	Ni(3)–N(21)	2.061(5)
Ni(1)–N(26)	2.031(5)	Ni(2)–N(12)	2.016(5)	Ni(3)–N(22)	1.977(5)
Ni(1)–N(35)	1.999(5)	Ni(2)–N(41)	2.052(5)	Ni(3)–N(45)	2.006(4)
Ni(1)–N(36)	2.075(5)	Ni(2)–N(42)	2.015(5)	Ni(3)–N(46)	2.077(6)
Ni(4)–S(1)	2.386(2)	Ni(4)–N(15)	1.983(5)	Ni(4)–N(31)	2.047(5)
Ni(4)–S(3)	2.395(2)	Ni(4)–N(16)	2.080(5)	Ni(4)–N(32)	1.993(5)
S(1)–C(8)	1.711(6)	C(8)–N(13)	1.288(8)	N(12)–N(13)	1.356(7)
		C(8)–N(14)	1.403(8)	N(14)–N(15)	1.361(7)
S(2)–C(23)	1.670(6)	C(23)–N(23)	1.347(8)	N(22)–N(23)	1.365(7)
		C(23)–N(24)	1.338(8)	N(24)–N(25)	1.360(7)
S(3)–C(38)	1.711(6)	C(38)–N(33)	1.393(8)	N(32)–N(33)	1.348(7)
		C(38)–N(34)	1.290(8)	N(34)–N(35)	1.370(7)
S(4)–C(53)	1.730(6)	C(53)–N(43)	1.296(7)	N(42)–N(43)	1.345(6)
		C(53)–N(44)	1.361(8)	N(44)–N(45)	1.338(7)
S(2)–Ni(1)–S(3)	94.2(1)	S(1)–Ni(2)–S(4)	94.2(1)		
Ni(1)–S(3)–Ni(4)	151.1(1)	Ni(2)–S(4)–Ni(3)	151.3(1)		
S(2)–Ni(3)–S(4)	94.9(1)	S(1)–Ni(4)–S(3)	95.1(1)		
Ni(1)–S(2)–Ni(3)	158.2(1)	Ni(2)–S(1)–Ni(4)	160.1(1)		

N(23) and N(24). The closest intermolecular distance between two HL^- ligands coordinated to different nickel centers is 3.65 Å, indicating weak π–π interactions. Though the stacking interactions are weak compared to the metal–nitrogen and metal–sulfur coordination bonds, this type of interactions is important in the assembly of the tetranuclear metal macrocyclic molecular square. Similarly, for complex **2** (Table 3) to make the refinement simpler, we added the hydrogen atoms riding on the nitrogen atoms N(23) and N(34), since the C–N bond distances, *ca.* 1.36 and 1.35 Å for C(23)–N(23) and C(38)–N(34), respectively, are of preferentially single bond character. The thiocarbazone hydrogen atom of the ligand containing S(4) was treated disordered over N(43) and N(44), since the C–N bonds (*ca.* 1.32 Å) in this ligand are intermediate between formal single and double bonds. The ligand containing S(1) is heavily disordered and bond distances were restrained, the thiocarbazone hydrogen atom is added disordered over C(13) and C(13′) to make the refinement simpler. The stacking interactions between ligands coordinated to different zinc centers were also found to stabilize the tetranuclear metal macrocyclic molecular square.

Magnetic properties of complexes 1 and 4

In the presence of metal ions having oxidation abilities, thiocarbazone derivatives may serve both as ligands and as reducing agents to give mixed valence compounds.[18] Reaction of bis(2-acetylpyridine) thiocarbazone with $FeCl_3$ gives a dark black precipitate. ESI-MS of the complex in methanol reveals the presence of a peak at *m*/*z* 732.2 assigned to the species $[Fe_4L_3(HL)]^{2+}$. It seems that such a complex should contain both Fe^{II} and Fe^{III}. In order to determine the molar ratio of Fe(II) and Fe(III), the temperature dependence of the molar magnetic susceptibility χ_m and the effective magnetic moment μ_{eff} for a polycrystalline sample of the tetranuclear complex **4** in the range of 75–300 K were carried out.The μ_{eff} *vs.* T plot for **4** is displayed in Fig. 3. The effective magnetic moment at room temperature of 10.48 μ_B, increases slightly with decreasing temperature and reaches 11.20 μ_B, the shapes of both curves are characteristic of very slightly ferromagnetic coupling among the iron ions. For comparison, the temperature dependence of the molar magnetic susceptibility χ_m and the effective magnetic moment μ_{eff} for a polycrystalline sample

Table 3 Selected bond lengths (Å) and angles (°) for complex $\mathbf{2}\cdot0.5H_2O$[a]

Zn(1)–S(2)	2.483(2)	Zn(2)–S(3)	2.476(2)	Zn(3)–S(1)	2.459(2)
Zn(1)–S(3)	2.470(2)	Zn(2)–S(4)	2.512(2)	Zn(3)–S(4)	2.520(2)
Zn(1)–N(25)	2.152(4)	Zn(2)–N(35)	2.111(4)	Zn(3)–N(11)	2.181(6)
Zn(1)–N(26)	2.122(5)	Zn(2)–N(36)	2.140(5)	Zn(3)–N(12)	2.189(6)
Zn(1)–N(31)	2.155(5)	Zn(2)–N(45)	2.115(4)	Zn(3)–N(41)	2.056(5)
Zn(1)–N(32)	2.125(4)	Zn(2)–N(46)	2.098(5)	Zn(3)–N(42)	2.115(4)
Zn(4)–S(1)	2.451(2)	Zn(4)–N(15)	2.198(6)	Zn(4)–N(21)	2.016(6)
Zn(4)–S(2)	2.514(2)	Zn(4)–N(16)	2.137(6)	Zn(4)–N(22)	2.123(4)
S(1)–C(8)	1.687(5)	C(8)–N(13)	1.349(11)	N(12)–N(13)	1.343(9)
		C(8)–N(14)	1.267(9)	N(14)–N(15)	1.367(10)
S(2)–C(23)	1.731(5)	C(23)–N(23)	1.365(7)	N(22)–N(23)	1.318(6)
		C(23)–N(24)	1.321(7)	N(24)–N(25)	1.349(6)
S(3)–C(38)	1.740(5)	C(38)–N(33)	1.259(7)	N(32)–N(33)	1.345(7)
		C(38)–N(34)	1.347(7)	N(34)–N(35)	1.399(6)
S(4)–C(52)	1.715(7)	C(52)–N(43)	1.321(6)	N(42)–N(43)	1.343(6)
		C(52)–N(44)	1.316(8)	N(44)–N(45)	1.331(5)
S(2)–Zn(1)–S(3)	97.0(1)	S(3)–Zn(2)–S(4)	94.9(1)		
Zn(1)–S(3)–Zn(2)	151.5(1)	Zn(2)–S(4)–Zn(3)	144.8(1)		
S(1)–Zn(3)–S(4)	100.3(1)	S(1)–Zn(4)–S(2)	102.3(1)		
Zn(3)–S(1)–Zn(4)	156.7(1)	Zn(1)–S(2)–Zn(4)	140.7(1)		

[a] Bond distances and angles of the major component of the disordered HL^- ligand are listed here.

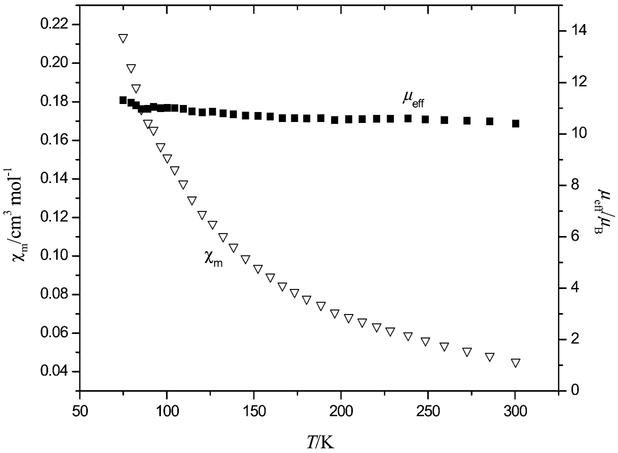

Fig. 3 Effective magnetic moment (μ_{eff}) and susceptibility χ_m data as a function of temperature for complex **4**.

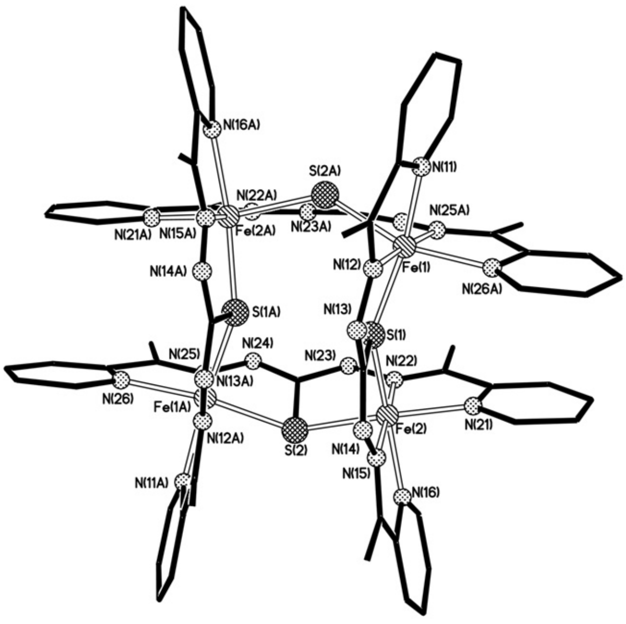

Fig. 4 Molecular structure showing one of the two tetranuclear cations $[Fe^{II}_3Fe^{III}L_2(HL)_2]^{3+}$. Symmetry code A: $-x$, y, $0.5 - z$.

of the tetranuclear complex **1**, in the range of 75–300 K were carried out. As the temperature is lowered, χ_m increases from 3.87×10^{-4} cm^3 mol^{-1} at room temperature and reaches a maximum of 3.02×10^{-3} cm^3 mol^{-1}. The effective magnetic moment at room temperature of 2.69 μ_B, which is very low compared to that expected for four independent Ni^{II} ions, decreases with decreasing temperature and reaches 0.48 μ_B at 75 K, indicating strong antiferromagnetic coupling among the Ni^{II} ions. Compared to the strong antiferromagnetic coupling among the metal centers in the nickel complex **1**, it is proposed that the tetranuclear square **4** might contain only one metal center with uncoupling electrons. Also the effective magnetic moment at room temperature of 10.48 μ_B is also consistent with three high spin Fe^{III} (contributed by three $FeCl_4^-$) and one low spin Fe^{III}; it seems that the iron-based square is in the form of $[Fe^{III}Fe^{II}_3(HL)_2(L)_2][FeCl_4]_3$.

Crystal structure of complex 4

There are two slight different halves of the molecular squares and three $FeCl_4^-$ anions are found in an asymmetric unit. Fig. 4 shows one of the two slightly different tetranuclear cations. The cations are located at inversion centers with four iron atoms at the corners of a square with edge length Fe···Fe *ca.* 4.2 Å, and S–Fe–S and Fe–S–Fe bond angles of *ca.* 96 and 145°, respectively. The C–S bond lengths of 1.77–1.80 Å (Table 4) are clearly indicative of single C–S bonds when compared to those of 1.70 to 1.74 Å in complexes **1** and **2**, indicating that the thiocarbazone moieties adopt thiol tautomeric form and act as mono-negative or double-negative ligands. Since there are three $Fe^{III}Cl_4^-$ anions in one asymmetry unit and only one low-spin state Fe^{III} was found in each cation, it is suggested that two of the four ligands are –2 charged anions and two −1 charged anions in each tetranuclear square cation. The C–N and N–N bond distances in the ligands are intermediate between formal single and double bonds, pointing to extensive delocalization over the entire molecular skeleton and to effects of disordered distribution of the protonated nitrogen sites in the ligand. Bond distances of 1.34 Å for C(23)–N(23) and C(38)–N(33) might be more single bond character than those of 1.30–1.32 Å for the other C–N bonds in thiocarbazone moieties, and as a consequence, N(23) and N(33) are treated as protonated in the crystal structure refine-

Table 4 Selected bond lengths (Å) and angles (°) for complex $\mathbf{4}\cdot H_2O\cdot 1.5C_6H_6$

Fe(1)–S(1)	2.159(2)	Fe(2)–S(1)	2.162(2)	Fe(3)–S(3)	2.260(2)
Fe(1)–S(2A)	2.264(2)	Fe(2)–S(2)	2.240(2)	Fe(3)–S(4A)	2.161(2)
Fe(1)–N(11)	1.976(6)	Fe(2)–N(15)	1.943(6)	Fe(3)–N(35)	1.931(6)
Fe(1)–N(12)	1.930(6)	Fe(2)–N(16)	1.985(6)	Fe(3)–N(36)	1.941(7)
Fe(1)–N(25A)	1.915(6)	Fe(2)–N(21)	1.955(6)	Fe(3)–N(45)	1.930(6)
Fe(1)–N(26A)	1.969(6)	Fe(2)–N(22)	1.929(6)	Fe(3)–N(46)	1.975(6)
Fe(4)–S(3)	2.234(3)	Fe(4)–N(31)	1.953(7)	Fe(4)–N(41)	1.988(6)
Fe(4)–S(4)	2.165(2)	Fe(4)–N(32)	1.939(7)	Fe(4)–N(42)	1.934(6)
S(1)–C(8)	1.800(7)	C(8)–N(13)	1.320(9)	N(12)–N(13)	1.376(8)
		C(8)–N(14)	1.311(9)	N(14)–N(15)	1.368(8)
S(2)–C(23)	1.768(7)	C(23)–N(23)	1.339(8)	N(22)–N(23)	1.367(8)
		C(23)–N(24)	1.300(9)	N(24)–N(25)	1.391(8)
S(3)–C(38)	1.785(8)	C(38)–N(33)	1.345(10)	N(32)–N(33)	1.344(9)
		C(38)–N(34)	1.297(10)	N(34)–N(35)	1.405(9)
S(4)–C(53)	1.783(7)	C(53)–N(43)	1.312(9)	N(42)–N(43)	1.382(8)
		C(53)–N(44)	1.324(9)	N(44)–N(45)	1.372(8)
S(1)–Fe(1)–S(2A)		95.8(1)	S(1)–Fe(2)–S(2)	97.0(1)	
Fe(1)–S(1)–Fe(2)		147.8(1)	Fe(1A)–S(2)–Fe(2)	133.6(1)	
S(3)–Fe(3)–S(4A)		95.32(9)	S(3)–Fe(4)–S(4)	97.3(1)	
Fe(3)–S(3)–Fe(4)		134.5(1)	Fe(3A)–S(4)–Fe(4)	148.1(1)	

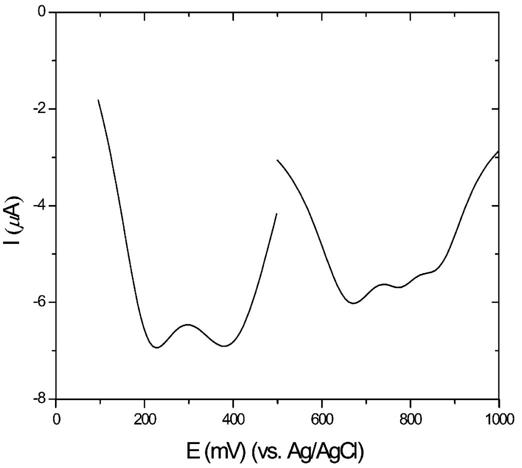

Fig. 5 Pulse voltammetry measurement of the complex **4** in acetonitrile solution containing 0.1 M tetrabutylammonium perchlorate as supporting electrolyte at a scan rate of 30 mV s^{-1}.

ment. There are no significant differences of the coordinated bonds among the four iron centers, indicating that is impossible to recognize the Fe^{III} in the four iron centers of a square.

Mixed-valence properties

Pulse voltammetry measurement of complex **4** (Fig. 5) exhibits five peaks at 0.23, 0.38, 0.67, 0.78 and 0.89 V. The peak corresponding to the $Fe^{III}Cl^{-}_4/Fe^{II}Cl^{-}_4$ oxidation appears at 0.23 V. As expected, the mixed-valence $[Fe^{II}_3Fe^{III}L_2(HL)_2]^{3+}$ cation undergoes four sequential one electron oxidations [eqn. (1)].

$$Fe^{II}_4 \xrightleftharpoons{-e} Fe^{II}_3Fe^{III} \xrightleftharpoons{-e} Fe^{II}_2Fe^{III}_2 \xrightleftharpoons{-e} Fe^{II}Fe^{III}_3 \xrightleftharpoons{-e} Fe^{III}_4 \quad (1)$$

The separation between the potentials for the first and second steps (0.29 V) is larger than the others, suggesting that $Fe^{III}Fe^{II}_3$ is the most stable species of the five species. Intervalence metal–metal interactions of complex **4**, verified by the information of intervalence transition (IT) band[19] in the UV–VIS–NIR spectrum (Fig. 6), shows one broad band at 1237 nm ($\varepsilon = 2410$ M^{-1} cm^{-1}). When the results derived by Hush[20] for mixed-valence complexes are applied to the Fe^{III}-Fe^{II}_3 species, $\nu_{max} = 8084$ cm^{-1} and $\Delta\nu_{1/2} = 2162$ cm^{-1}) with the iron–iron distance (4.2 Å) taken from the X-ray data, they lead to a degree of electronic delocalization (α^2) of 0.0155 and the interaction energy (H_{rp}) is 1006 cm^{-1}. The degree of delocalization indicates Robin–Day class II behavior.[21] Such electron transfer process model systems in which the electron moves between chemically equivalent sites where it is weakly trapped are very valuable in chemistry, physics and biology.[22]

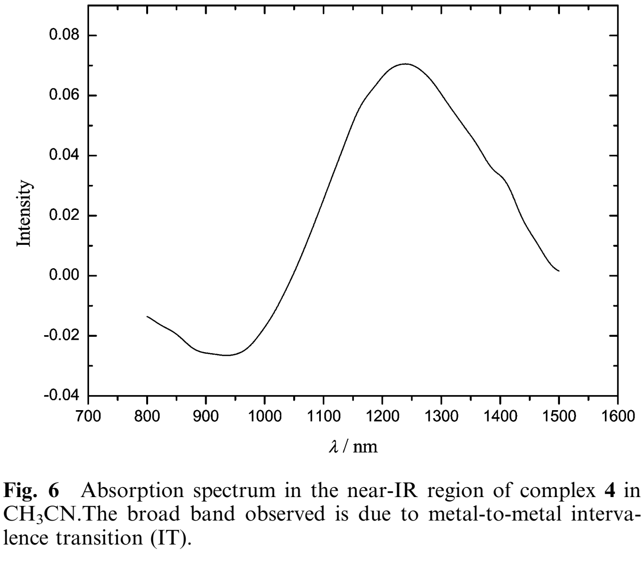

Fig. 6 Absorption spectrum in the near-IR region of complex **4** in CH_3CN.The broad band observed is due to metal-to-metal intervalence transition (IT).

Acknowledgements

This work was supported by the National Natural Science Foundation of China. We also thank Mr Liu Yong-jiang for collecting the crystal data and Ms Mei Yu-hua for measuring the ESI-MS spectra.

References

1 (*a*) R. V. Slone, K. D. Benkstein, S. Belanger, J. T. Hupp, I. A. Guzei and A. L. Rheingold, *Coord. Chem. Rev.*, 1998, **171**, 221; (*b*) S. Bélanger, J. T. Hupp, C. L. Stern, R. V. Slone, D. F. Watson and T. G. Carrell, *J. Am. Chem. Soc.*, 1999, **121**, 557; (*c*) S. S. Sun and A. J. Lees, *Inorg. Chem*, 1999, **38**, 4181.

2 (*a*) F. S. McQuillan, T. E. Berridge, H.-L. Chen, T. A. Hamor and C. J. Jones, *Inorg. Chem.*, 1998, **37**, 4959; (*b*) C. J. Matthews, Z. Q. Xu, S. K. Mandal, L. K. Thompson, K. Biradha, K. Poirier and M. J. Zaworotko, *Chem. Commun.*, 1999, 347; (*c*) M. Lahav, R. Gabai, A. N. Shipway and I. Willner, *Chem. Commun.*, 1999, 1937

3 (*a*) E. Solari, W. Lesueur, A. Klose, K. Schenk, C. Floriani, A. Chiesi-Villa and C. Rizzoli, *Chem. Commun.*, 1996, 807; (*b*) I. M. Atkinson, C. Benelli, M. Murrie, S. Parsons and R. E. P. Winpenny, *Chem. Commun.*, 1999, 285; (*c*) E. Colacio, C. Lopez-Magana, V. McKee and A. Romerosa, *J. Chem. Soc., Dalton Trans.*, 1999, 2923.

4 G. F. Swiegers and T. J. Malefetse, *Chem. Rev.*, 2000, **100**, 3483.

5 (*a*) E. Breuning, M. Ruben, J.-M. Lehn, F. Renz, Y. Garcia, V. Ksenofontov, P. Gütlich, E. Wegelius and K. Rissanen, *Angew. Chem., Int. Ed.*, 2000, **39**, 2504; (*b*) K. D. Benkstein, J. T. Hupp and C. L. Stern, *Angew. Chem., Int. Ed.*, 2000, **39**, 2891.

6 (*a*) J. Fan, J. A. Whiteford, B. Olenyuk, M. D. Levin, P. J. Stang and E . B. Fleischer, *J. Am. Chem. Soc.*, 1999, **121**, 2741; (*b*) L. Pan, B. C. Noll and X.-T. Wang, *Chem. Commun.*, 1999, 157; (*c*) C. M. Drain, F. Nifiatis, A. Vasenko and J. D. Batteas, *Angew. Chem., Int. Ed.*, 1998, **37**, 2344; (*d*) X. Chi, A. J. Guerin, R. A. Haycock, C. A. Hunter and L. D. Sarson, *J. Am. Chem. Soc. Chem. Commun.*, 1995, 2567.

7 (*a*) C. Y. Duan, Z. H. Liu, X. Z. You, F. Xue and T. C. W. Mak, *Chem. Commun.*, 1997, 381; (*b*) C. He, C. Y. Duan, C. J. Fang, Y. J. Liu and Q. J. Meng, *J. Chem. Soc., Dalton Trans.*, 2000, 1207; (*c*) C. J. Fang, C. Y. Duan, D. Guo, C. He and Q. J. Meng, *Chem. Commun.*, 2001, 2540.

8 (*a*) S. B. Pödhye and G. B. Kauffman, *Coord. Chem Rev.*, 1985, **63**, 127; (*b*) A. Liberta and D. X. West, *Biometals*, 1992, **5**, 121; (*c*) E. Lukevics, D. Jansone, K. Rubina, E. Abele, S. Germane, L. Leite, M. Shymanska and J. Popelis, *Eur. J. Med. Chem.*, 1995, **30**, 983.

9 (*a*) M. B. Ferrari, G. G. Fava, P. Tarasconi, R. Albertin,Pinelli and R. Starcich, *J. Inorg. Biochem.*, 1994, **53**, 13; (*b*) J. G. Cory, A. H. Cory, G. Rappa, A. Lorico, M. C. Liu and A. S. Sartorelli, *Biochem Pharmacol*, 1994, **48**, 335; (*c*) M. C. Liu, T. S. Lin, P. Penketh and A. S. Sartorelli, *J. Med. Chem.*, 1995, **38**, 4234.

10 (*a*) D. X. West, S. B. Pödhye and P. B. Sonawane, *Struct. Bonding (Berlin)*, 1991, **76**, 1; (*b*) S. B. Turk, C. Shipman and J. C. Drach, *Biochem. Pharmacol.*, 1986, **35**, 1539; (*c*) B. G. Choi, *Yakhak Hoechi*, 1986, **30**, 79; (*d*) T. A. Blumenkopf, J. A. Harrington, C. S. Koble, D. D. Bankston, R. W. Morrison, E. C. Bigham, V. L. Styles and T. Spector, *J. Med. Chem.*, 1992, **35**, 2306.

11 (*a*) Z. H. Liu, C. Y. Duan, J. Hu and X. Z. You, *Inorg. Chem.*, 1999, **38**, 1719; (*b*) Y. P. Tian, C. Y. Duan, Z. L. Lu, X. Z. You, T. C. W. Mak and Z. Y. Zhang, *Inorg. Chem.*, 1997, **36**, 1247; (*c*) Z. H. Liu, C. Y. Duan, J. H. Li, Y. J. Liu, Y. H. Mei and X. Z. You, *New J. Chem.*, 2000, 1057.

12 (*a*) B. Moubaraki, K. S. Murray, J. D. Ranford, J. J. Vittal, X. Wang and Y. Xu, *J. Chem. Soc., Dalton Trans.*, 1999, 3573; (*b*) B. Moubaraki, K. S. Murray, J. D. Ranford, X. Wang and Y. Xu, *Chem. Commun.*, 1998, **353**; (*c*) A. Bacchi, A. Bonini, M. Carcelli, F. Ferraro, E. Leporati, C. Pelizzi and G. Pelizzi, *J. Chem. Soc., Dalton Trans.*, 1996, 2699.

13 (*a*) R. B. King, *Encyclopendia of Inorganic Chemistry*, Chichester–New York: 1994, p. 2270; (*b*) W. P. Fehlhammer and M. Fritz, *Chem. Rev.*, 1993, **93**, 1243; (*c*) C. Creatz, *Prog. Inorg. Chem.*, 1983, **30**, 1.

14 (*a*) S. B. Piepho, *J. Am. Chem. Soc.*, 1990, **112**, 4197; (*b*) A. L. Feig and S. J. Lippard, *Chem. Rev.*, 1994, **94**, 759; (*c*) K. L. Taft, G. C. Papaefthymiou and S. J. Lippard, *Science*, 1993, **259**, 1302.

15 (*a*) M. DiVaira, F. Mani and P. Stoppioni, *J. Chem. Soc., Dalton Trans.*, 1997, 1375; (*b*) M. Beley, S. Chodorowski and J. P. Collin, *Angew. Chem., Int. Ed. Engl.*, 1994, **33**, 1775; (*c*) G. U. Bublitz, W. M. Laidlaw, R. G. Denning and S. G. Boxer, *J. Am. Chem. Soc.*, 1998, **120**, 6068.

16 SMART and SAINT. Area Detector Control and Integration Software. Siemens Analytical X-Ray Systems, Inc., Madison, Wisconsin, USA, 1996.

17 G. M. Sheldrick, SHELXTL V5. 1, Software Reference Manual, Bruker AXS, Inc., Madison, WI, USA, 1997.

18 (*a*) Z. H. Liu, S. Y. Yang, C. Y. Duan and X. Z. You, *Chem. Lett.*, 1999, 1063; (*b*) M. Dunaj-Jurčo, G. Ondrejovič and M. Melník, *Coord. Chem. Rev.*, 1988, **83**, 1.

19 B. W. Pfenning, J. L. Cohen, I. Sosnowski, N. M. Novotny and D. M. Ho, *Inorg. Chem*, 1999, **38**, 606.

20 (*a*) N. S. Hush, *Prog. Inorg. Chem.*, 1967, **8**, 391; (*b*) W. M. Laidlaw and R. G. Denning, *J. Chem. Soc., Dalton Trans.*, 1994, 1987.

21 M. B. Robin and P. Day, *Adv. Inorg. Chem. Radiochem.*, 1967, **10**, 247.

22 C. Stadler, J. Daub, J. Köhler, R. W. Saalfrank, V. Coropceanu, V. Schünemann, C. Ober, A. X. Trautwein, S. F. Parker, M. Poyraz, T. Inomata and R. D. Cannon, *J. Chem. Soc., Dalton Trans.*, 2001, 3373.